Negative wake behind a sphere rising in viscoelastic fluids: A lattice Boltzmann investigation

Xavier Frank and Huai Z. Li*

Laboratoire des Sciences du Génie Chimique (CNRS, UPR 6811), ENSIC-INPL, 1, rue Grandville, Boîte Postale 20451, 54001 Nancy Cedex, France

(Received 10 April 2006; revised manuscript received 7 August 2006; published 28 November 2006)

We investigate the complex flow field around a sphere rising in a Maxwell fluid by means of the lattice Boltzmann simulation to provide insights into the strange negative wake experimentally observed behind a bubble or particle in non Newtonian fluids. The influence of the rise velocity, sphere diameter, and fluid's rheology is considered through two dimensionless numbers: the Deborah number De and the Reynolds number Re. Our simulation shows that the negative wake appears behind the sphere when $De>2$. On the other hand, the shape of the negative wake described by the opening angle θ of the upward flow cone surrounding the negative wake is mainly determined by the Reynolds number Re. These results reveal that the physical origin of the negative wake stems mainly from the competition between the elastic and viscous stresses in the fluid.

DOI: 10.1103/PhysRevE.74.056307 PACS number(s): 47.50.−d, 47.55.D−, 47.11.−j

INTRODUCTION

The motion of an isolated bubble in fluids has been the focus of both academic and industrial interest, and attracted the attention of scientists for a long time [1]. Compared to bubbles in Newtonian fluids, much less is known about the bubble behavior in non-Newtonian fluids. In particular, the fundamental physical mechanism remains unclear concerning some peculiar phenomena not observed in Newtonian fluids such as the so-called negative wake shown by laser Doppler anemometry [2], the complete wake with both a negative wake and an upward flow cone obtained by particle image velocimetry (PIV) [3], as well as the memory effects in stress relaxation in bubble coalescence [4]. Due to the inherent complex nature of bubble phenomena and the influence of the fluid's rheology, an exhaustive theoretical analysis is still beyond reach at present. Since the pioneering work [5], the main contributions in the literature have been devoted to both the experimental measurements of the bubble rise velocity in such fluids and the visual observation.

In the past, several numerical studies [6–13] have also been performed for the flow past spheres in viscoelastic fluids by means of different numerical methods, such as finite-element analysis and distributed Lagrange multiplier methods. These computations concern mainly the typical constitutive equations like the Chilcott-Rallison version of the Finitely Extensible Nonlinear Elastic (FENE-CR) dumbbell or Oldroyd-B models with a relatively limited Deborah number De. In particular, the numerical results raise the recurring question of why negative wakes occur in some polymeric fluids while others show the opposite behavior. One suggestion is that both shear thinning and elasticity would be necessary for the formation of a negative wake. Also, shear properties alone cannot explain some experimental observations [9] that fluids with similar shear properties can show widely different wake profiles.

The present work aims at gaining insight into the physical origin of the complex wake phenomena behind an isolated bubble rising in a non-Newtonian fluid. The lattice Boltzmann (LB) approach is developed to explore computationally the interesting and so far unexplained role of interactions between rheological effects and inertial effects on the wake structure by means of a simple linear rheological equation.

I. PREVIOUS RESULTS

Early experiments on polymer solutions revealed a remarkable viscoelastic flow phenomenon, termed a negative wake [2]. The fluid behind the bubble moves downward, in the opposite direction to the rising bubble. This intriguing flow pattern was also reported for rigid spheres falling through a viscoelastic fluid [14,15]. These experiments were mainly carried out with a laser Doppler anemometer that provides a partial flow field at a point in fluid. Recently, the development of the PIV technique has allowed one to obtain a complete two- (2D) or three-dimensional (3D) flow field in a measurement window. In the case of the rise of a bubble through a viscoelastic fluid that is an axisymmetric flow, Funfschilling and Li revealed, by using a PIV device, that the 2D flow field around a bubble in such media is quite complex indeed [3]. In front of the bubble, the flow field is upward and similar to that in a Newtonian fluid due to the ascension of the bubble. The strangest feature of the flow field is the negative wake that occurs just behind the bubble. Around this negative wake, the fluid flow is upward with a conical shape (Fig. 1). It is thus possible to determine the open angle θ of the upward cone to characterize the flow pattern (Fig. 1). Moreover, our previous experiments show that θ decreases with increasing Reynolds number Re. In particular, θ is close to 180° for small values of Re.

The fundamental origin of the negative wake remains unclear up to now. Contradictory results between different authors in the literature contribute also to keeping alive this mystery. One possible suggestion is that the negative wake occurs in shear-thinning and elastic fluids. Our recent LB simulations performed with a nonlinear rheological model and the free-energy-based diphase scheme led to a good agreement with experiments for flow field, bubble shape, and stress field [16]. However, due to the complex nature of the

*Electronic address: li@ensic.inpl-nancy.fr

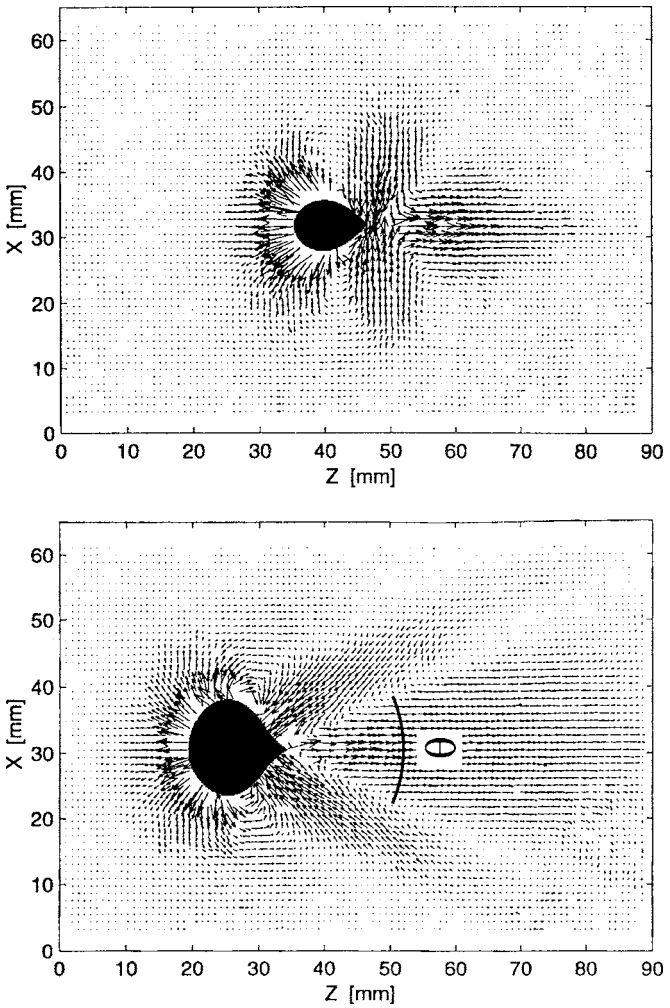

FIG. 1. Experimental PIV measurement of the flow field around a bubble in 0.75% polyacrylamide solution. Left: bubble volume $V_0=250$ mm^3, the Reynolds number based on the zero shear rate viscosity Re=0.01. Right: bubble volume $V_0=1200$ mm^3, Re =0.05. Real bubble shapes are added.

rheological model for describing the fluids, the contribution to the negative wake cannot be clearly divided between the nonlinear elasticity and viscous shear-thinning effects. In addition, the specific elongated shape of bubbles in such media could play a role in this flow pattern.

In the present work, we focus on the physical understanding of the negative wake by considering simply a linear rheological equation for the fluid and neglecting the bubble's shape evolution. Thus, the flow is only induced by the rise of a sphere in a 2D column. We consider then the rise of a sphere of diameter d_B with a rise velocity u_B. The 2D column has a width of ζd_B and a height of $\epsilon\zeta d_B$, where ζ and ϵ are simple multiplication factors. As shown in the following validation section, $\zeta=10$ and $\epsilon=2$ are found as a suitable compromise solution between minimizing wall effects and having a reasonable computation time. To define equations in dimensionless form, we choose d_B as the characteristic length and u_B as the reference velocity.

It is worth noting that stress boundary conditions for a solid sphere are not the same as for a bubble. To eliminate the possible contribution from both the deformable interface of a bubble and the stress-free boundary conditions to the negative wake, simple no-slip boundary conditions for a solid sphere are implemented in our simulations.

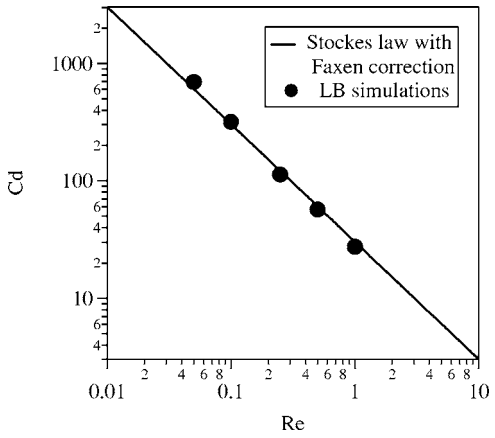

FIG. 2. Comparison of the drag coefficient between the Stokes equation modified by the Faxen correction and our LB simulations.

II. MACROSCOPIC EQUATIONS

For the sake of generality, we express the equations of the fluid with dimensionless numbers. First, the basic equation is the classical Navier-Stokes equation

$$\frac{\partial \vec{u}}{\partial t} + (\vec{u}\cdot\vec{\nabla})\vec{u} = -\vec{\nabla}P + \vec{\nabla}\cdot\Gamma. \tag{1}$$

If we define the shear rate tensor $D_{i,j}=\partial u_i/\partial x_j+\partial u_j/\partial x_i$, deduced from the finite-difference scheme, the stress tensor Γ, within the framework of the Maxwell model, is described by the linear equations

$$\frac{\partial \Gamma}{\partial t} + (\vec{u}\cdot\vec{\nabla})\Gamma = -\frac{1}{\mathrm{De}}(\Gamma-\Gamma^{eq}), \tag{2}$$

$$\Gamma^{eq} = \frac{1}{\mathrm{Re}}D. \tag{3}$$

We define the Deborah number De by $\mathrm{De}=\lambda u_B/d_B$ and the Reynolds number as $\mathrm{Re}=\rho_L d_B u_B/\eta$ where λ is the characteristic time of the fluid. If the advection term $(\vec{u}\cdot\vec{\nabla})\Gamma$ is neglected, we obtain then the simple Maxwell equation

$$\frac{\partial \Gamma}{\partial t} = -\frac{1}{\mathrm{De}}(\Gamma-\Gamma^{eq}). \tag{4}$$

A linear constitutive equation could seem to be too simple with respect to a real non-Newtonian fluid. However, such an approach is not rare in the literature [17]. Our previous studies on the mechanism governing the in-line interactions and coalescence between bubbles in non-Newtonian fluids have shown that such an equation can satisfactorily capture the large experimental wealth of data about the dynamical competition between the creation of stresses after the passage of bubbles and their relaxation, displaying temporarily a re-

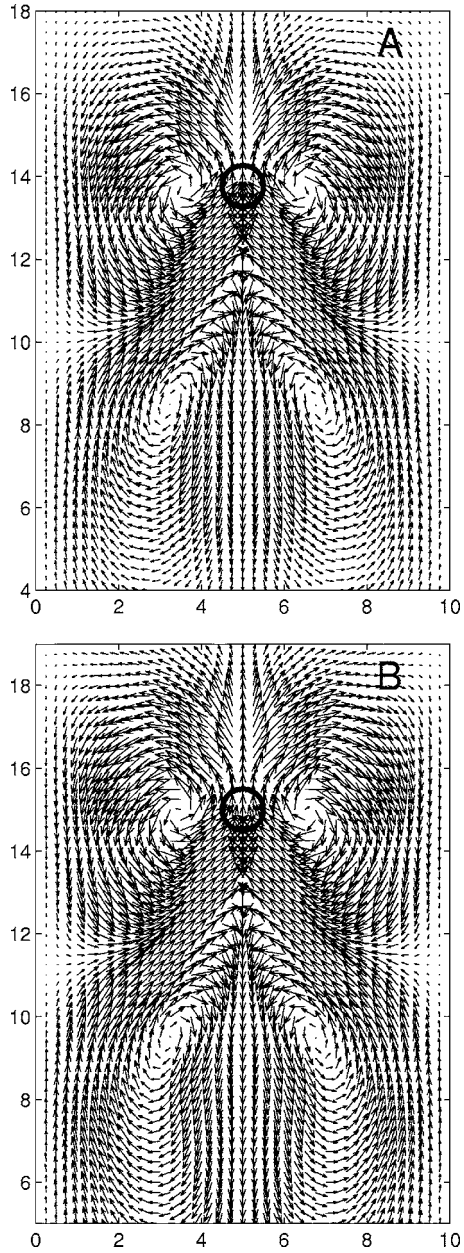

FIG. 3. LB simulations with De=10 and Re=0.4 with advection. (a) Fixed sphere and sliding walls; (b) rising sphere and fixed walls.

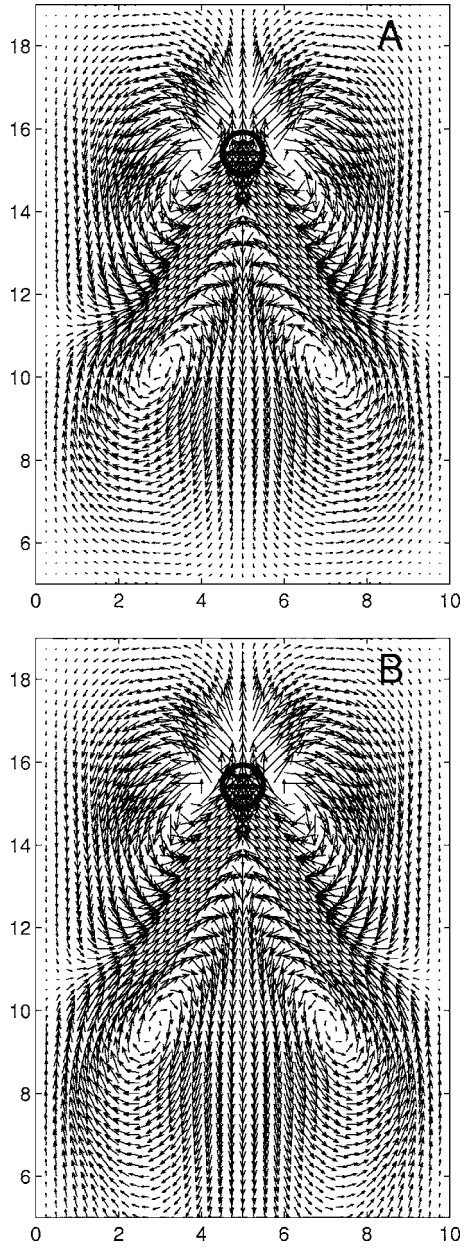

FIG. 4. LB simulations with De=10 and Re=0.4 without advection, rising sphere and fixed walls. (a) 200×400 nodes; (b) 400×800 nodes.

duced viscosity [18]. Moreover, the use of a linear equation can also avoid the trap of the contradictory results in the literature which could arise from the nonlinearity of the rheological equations. From a fundamental point of view, if we demonstrate the existence of a negative wake even with such a simple constitutive equation, we can exclude then the possible numerical artifact due to the interference of a complex nonlinear equation of rheology.

III. APPLICATION OF THE LATTICE BOLTZMANN METHOD

For a decade, the LB method has emerged from nonequilibrium statistical physics to become an alternative numerical method in fluid dynamics [19–22]. In contrast, the extension of the LB simulation to non-Newtonian flows has received limited attention so far, as mentioned in [23].

To perform the numerical simulation of the rise of a sphere in a viscoelastic fluid, the Navier-Stokes equation is not explicitly implemented in our LB scheme. In fact, the fluid motion is described by a particle probability density function (PPDF) f_i. Particles are forced to jump from a node of the lattice to a neighboring one, which can be done only with the velocities $\vec{c}_i$ that define, with the node positions, the lattice. In such a way, f_i is, at one point, the number of particles having the velocity $\vec{c}_i$. The main relevant hydrodynamic quantities are expressed as functions of the momenta of f_i,

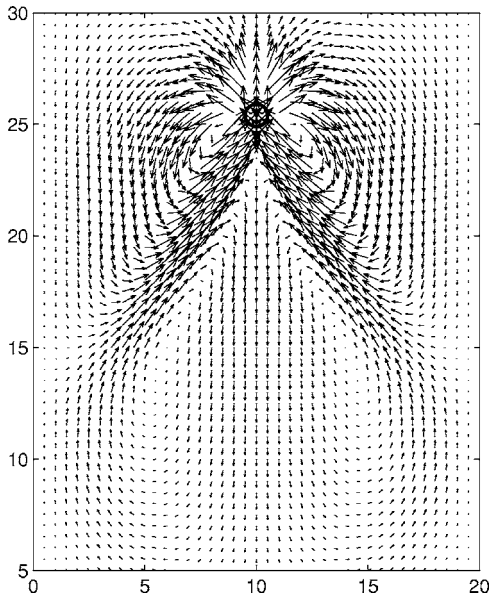

FIG. 5. LB simulations with De=10 and Re=0.4 without advection, rising sphere, fixed walls, and larger column. $\zeta=20$ and $\mathrm{Re}_{\mathrm{LB}}=10$.

$$\rho = \sum_i f_i, \tag{5}$$

$$\rho u_\alpha = \sum_i f_i c_{i\alpha}. \tag{6}$$

We use a classical D2Q9 lattice which is a two-dimensional lattice involving nine velocities. The lattice Bhatnagar-Gross-Krook equation, which is an approximation of the general LB equation, can be written as follows:

$$f_i(\vec{r}+\delta t\vec{c}_i, t+\delta t) - f_i(\vec{r},t) = -\omega(f_i - f_i^{eq}). \tag{7}$$

Intrinsically, the LB scheme involves purely viscous stresses that are superimposed on viscoelastic stresses Γ. To compare their importance to the inertia, we can define a lattice Boltzmann Reynolds number Re_{LB} that is linked to the frequency parameter ω and time step δt as $\delta t=(\mathrm{Re}_{LB}\delta x^2/3)\times(1/\omega-1/2)$. We choose here to fix $\mathrm{Re}_{LB}=10$ in order to limit the influence of pure LB viscous stresses [24].

Macroscopic quantities such as mass and momentum are used to compute the equilibrium values f_i^{eq} in the form of polynomial expressions. The momenta of these distributions obey

$$\sum_i f_i^{eq} = \rho, \tag{8}$$

$$\sum_i f_i^{eq} c_{i\alpha} = \rho u_\alpha, \tag{9}$$

$$\sum_i f_i^{eq} c_{i\alpha} c_{i\beta} = \rho u_\alpha u_\beta + \rho {c_s}^2 \delta_{\alpha\beta} - \Gamma_{\alpha\beta}, \tag{10}$$

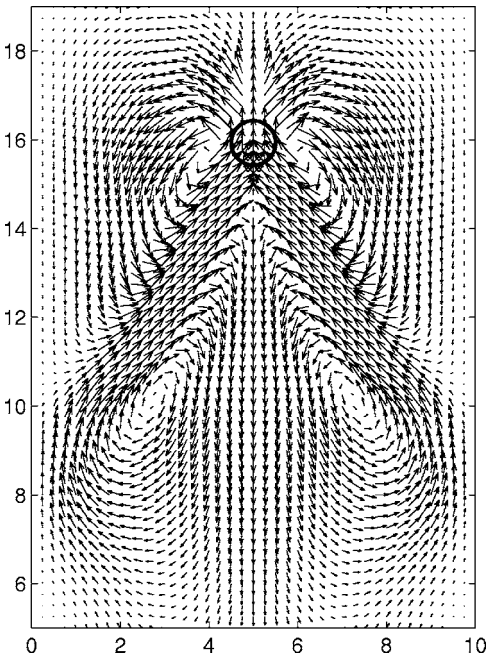

FIG. 6. LB simulations with De=10 and Re=0.4 without advection, rising sphere and fixed walls. $\zeta=10$ and $\mathrm{Re}_{\mathrm{LB}}=24$.

$$\sum_i f_i^{eq} c_{i\alpha} c_{i\beta} c_{i\gamma} = \frac{\rho}{3}(u_\gamma \delta_{\alpha\beta} + u_\alpha \delta_{\gamma\beta} + u_\beta \delta_{\alpha\gamma}). \tag{11}$$

The viscoelasticity is included by modifying the equilibrium distribution equation as shown in (10). Another implementation of the viscoelastic stress in a LB framework was proposed by Giraud *et al.* [25]. These authors added two distributions f_i to the PPDF in order to establish a linear relationship between the 11 PPDFs and all macroscopic significant quantities, including the viscoelastic stress tensors. With LB relaxation times depending upon i, it is then possible to make use of the Jeffreys rheological model. Such an approach was applied to the computation of the shape of a bubble rising in a viscoelastic fluid [26], but without information about the flow field.

We introduce the rise of a sphere by modifying the velocity expression:

$$\rho u_\alpha = (1-\Phi)\sum_i f_i c_{i\alpha} + \Phi \rho u_{B\alpha}. \tag{12}$$

The index Φ is computed for each time step as the position of the sphere changes. To avoid numerical instability, the sphere's rise velocity $\vec{u_B}$ is progressively increased up to a stationary value. The value $\Phi=1$ means inside the sphere and $\Phi=0$ outside the sphere.

IV. VALIDATION

To validate the implementation of such boundary conditions, we performed the simulations of a solid sphere settling down in cylinders of varying diameters. The computed drag coefficient C_d for different Reynolds numbers Re compares satisfactorily with the well-known Stokes equation modified

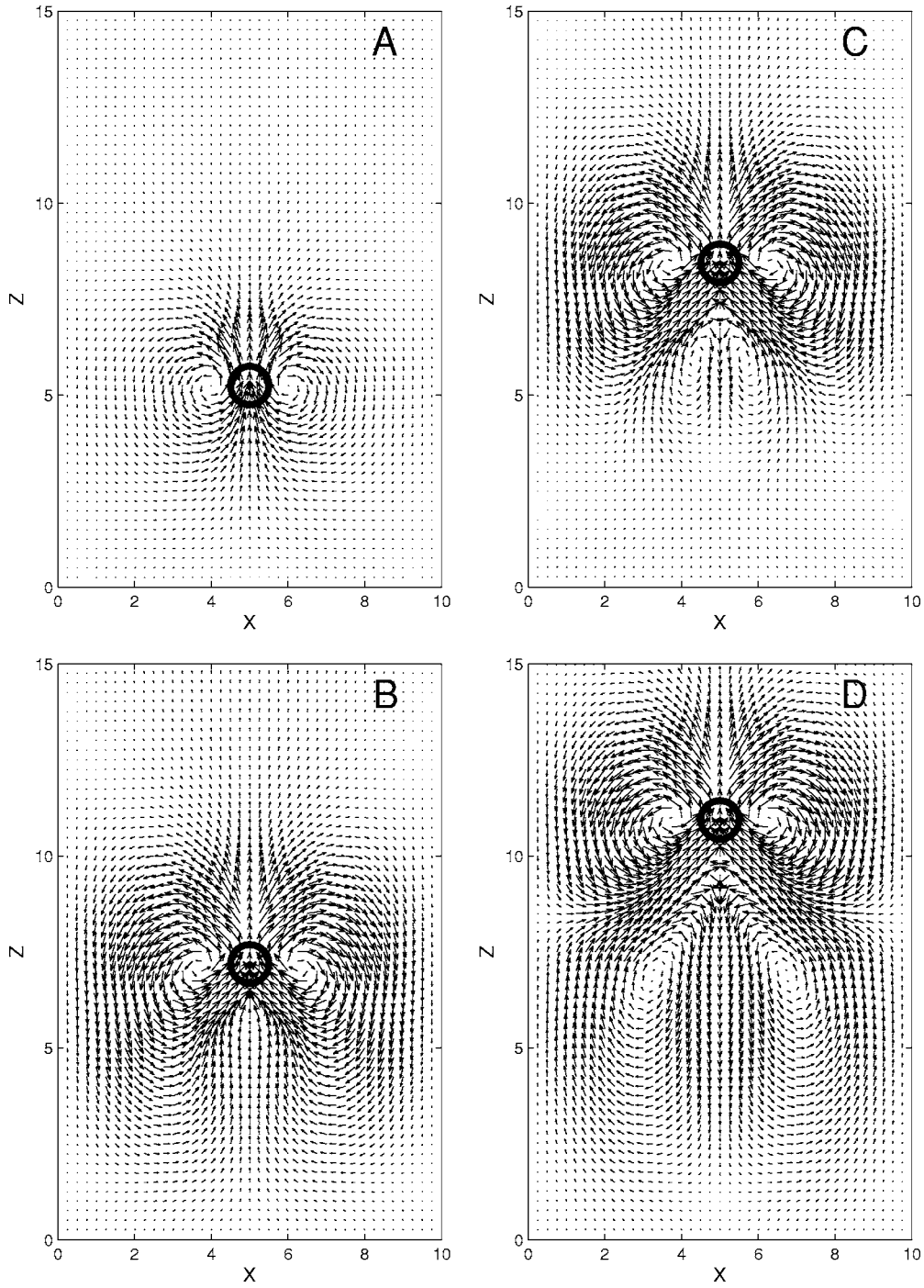

FIG. 7. LB simulations with De=10 and Re=0.2 in the transient regime at time t=(a) 1.25, (b) 3.75, and (c)=5.00; (d) at time t =7.50 in the stationary flow regime.

by Faxen's correction due to the wall effect (Fig. 2).

To check the possible advection effects, we performed consecutively three numerical tests under varying De and Re values. First, we used Eq. (2) for the flow field around a fixed sphere with the walls moving downward. Second, the simulation was conducted for a rising sphere with fixed walls. As there is no significant difference between the first simulation and the second one (Fig. 3), the Galilean invariance of Eq. (2) seems to be respected within the conditions for our simulation.

Finally, we used the simple Maxwell equation without advection (4) for a rising sphere with the walls at rest. Moreover, the similar results obtained by the third simulation with respect to the first and second ones tend to confirm that the advection plays only a minor role in the walls' reference frame.

For these reasons, we adopt finally the simple Maxwell model (4). Our model is grid convergent as simulations were tested with lattices of respectively 200×400, 300×600, and 400×800 nodes (Fig. 4).

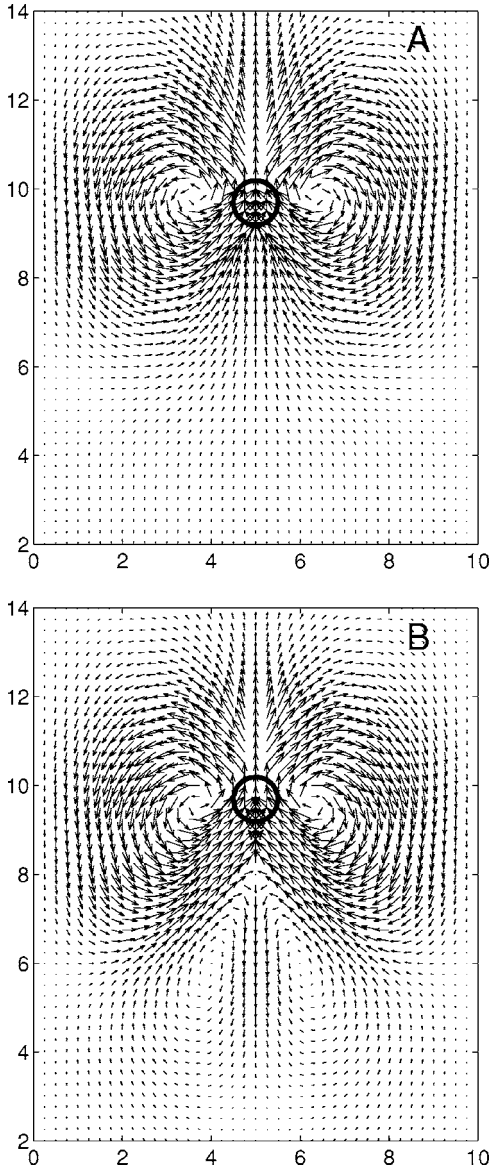

FIG. 8. Simulated flow fields around a sphere rising in a simple Maxwell fluid for Re=0.5; De=(a) 1.0 and (b) 5.0.

The definition of the 2D column is based on the sphere's diameter d_B: width of ζd_B and height of $\epsilon\zeta d_B$. To verify the possible role of the side walls in the flow around the rising sphere, several numerical experiments were conducted with different values of ζ for the width of the column. Clearly, limited widths of the column (for $\zeta<8$) do affect the flow picture. In addition to the heavy computation, very high values of ζ were not found necessary to conserve the flow fields. A typical result with $\zeta=20$ is shown in Fig. 5. With respect to a smaller simulated flow area with $\zeta=10$ (Fig. 4), the fundamental characteristics of the flow, in particular, the negative wake behind the sphere, are significantly similar. Quantitatively, the cone angle of the negative wake is 57.0° for $\zeta=10$ and 55.5° for $\zeta=20$. We consider then the value of $\zeta=10$ large enough to avoid the effects of side walls.

Finally, the possible role of the numerical viscosity within the LB scheme was investigated in the present work through varying the value of the lattice Boltzmann Reynolds number Re_{LB}. Even with an excessively high value of $\mathrm{Re}_{LB}=24$ as shown in Fig. 6, the modification of the flow picture can be considered as negligible compared to the previous simulation with $\mathrm{Re}_{LB}=10$ (Fig. 4).

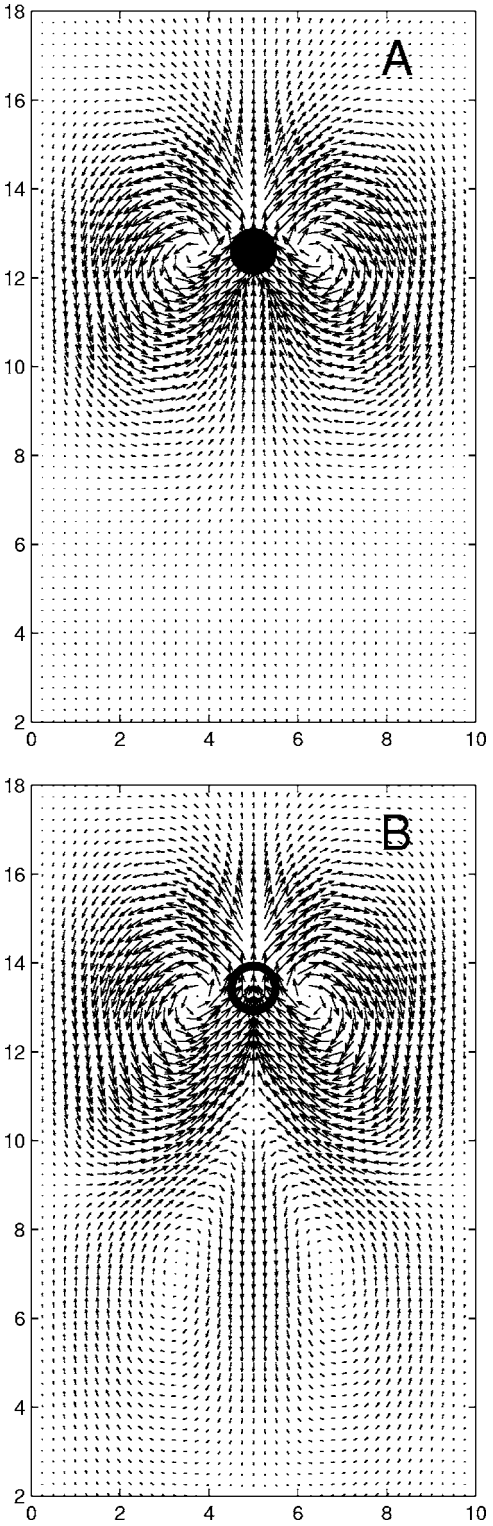

FIG. 9. Simulated flow fields around a sphere rising in a simple Maxwell fluid for Re=1.0. De=(a) 1.0 and (b) 5.0.

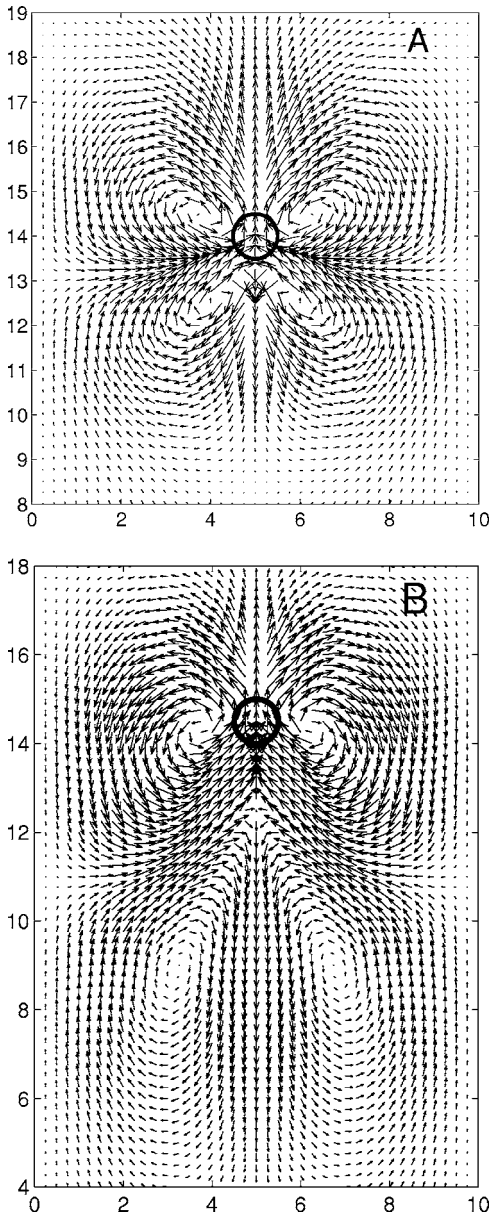

FIG. 10. Simulated flow fields around a sphere rising in a simple Maxwell fluid for De=10. Re=(a) 0.05 and (b) 0.4.

V. TRANSIENT FLOW FIELD

The numerical simulation is performed by accelerating progressively a sphere initially at rest to reach a stationary rise velocity u_B. The temporally evolution of the flow field can then be consecutively obtained. A typical example is illustrated in Fig. 7 showing the transient modification of the flow picture toward the establishment of a stationary flow regime with De=10 and Re=0.2.

As we can see in Fig. 7(a), the flow around the sphere at the beginning of the rise is quite similar to the Newtonian case. Progressively, a long wake appears behind the sphere as the fluid is increasingly deformed to produce significant viscoelastic stresses shown in Fig. 7(b). At a critical point, the central flow behind the sphere is suddenly reversed: the initial upward flow in the wake is pushed down to create the well-known negative wake surrounded by a conical upward flow [Fig. 7(c)]. Then, the negative wake and the upward cone become spatially more extended to reach finally the stationary flow field [Fig. 7(d)].

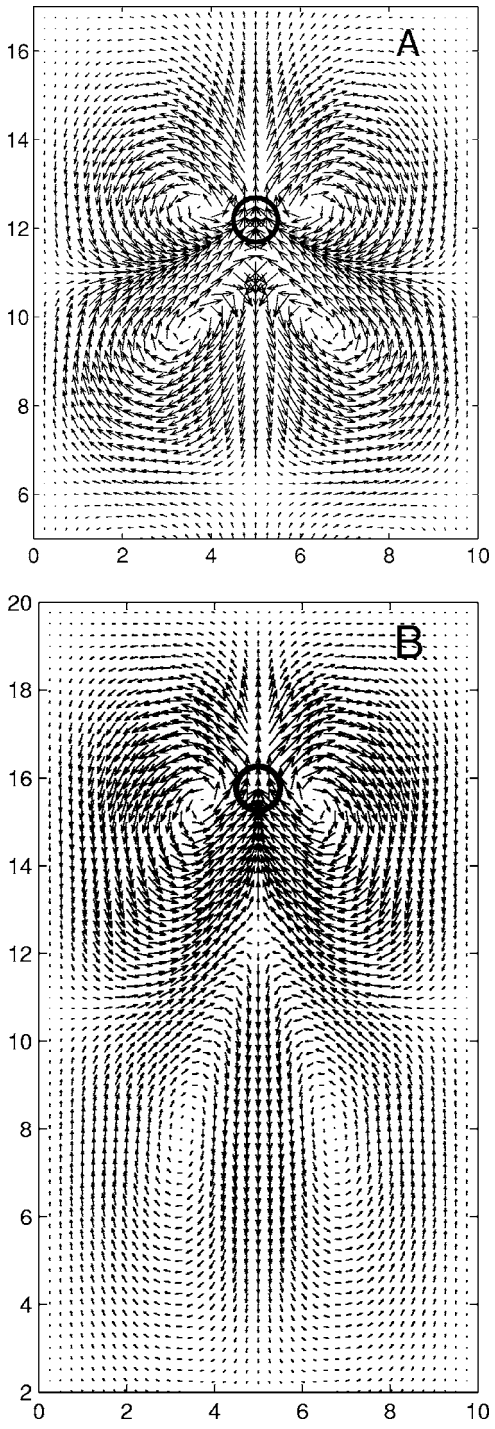

FIG. 11. Simulated flow fields around a sphere rising in a simple Maxwell fluid for De=20. Re=(a) 0.05 and (b) 0.5.

VI. TRANSITION TO THE NEGATIVE WAKE

First, we verify the influence of elastic stresses as a possible origin of the negative wake. These stresses are created

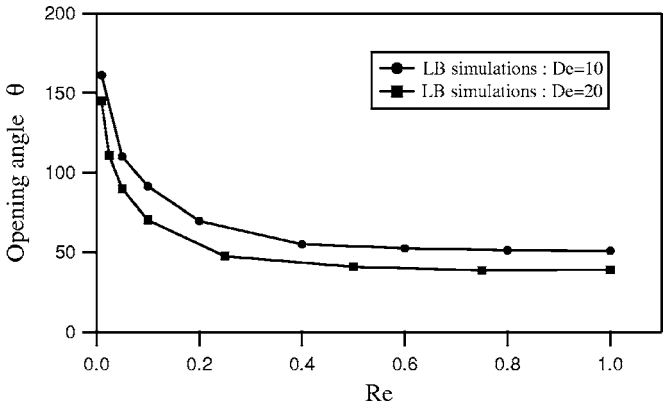

FIG. 12. Opening angle θ as a function of Re for De=10 and 20.

by the sphere passage, and relax in the wake behind the bubble. They are mainly described by the Deborah number De.

The LB simulations are performed under various Deborah numbers De ranging from 0.5 to 5 for two Reynolds numbers Re=0.5 and 1.0.

As shown in Figs. 8 and 9, the negative wake occurs for De$>$2. For De$<$2, the flow is quite close to that in Newtonian viscous flows, as the relaxation of viscoelastic stresses is faster than their generation by the shear due to the passage of the sphere. On the other hand, the competition between these two antagonistic mechanisms moves in favor of the stress relaxation when De$>$2 as viscoelastic stresses require a very long time to relax.

It is worth noting that the flow fields with high De values described by the LB simulations are in good qualitative agreement with our experimental measurements of bubbles rising in different polyacrylamide solutions by means of a 2D PIV device [3]. Certainly, the consideration of the bubble's shape as well as a nonlinear constitutive equation of rheology can lead to a better quantitative description of the flow field around a nonspherical bubble [16]. But the central question about the existence of the negative wake receives a satisfactory response from the key parameter, that is, the Deborah number De. The origin of the negative wake can be clearly attributed to the viscoelastic character of the fluid.

VII. OPENING ANGLE

To gain insight into the experimentally observed modulation of the opening angle θ, we consider the influence of the Reynolds number Re which depends mainly on the sphere's size and fluid's properties. The LB simulations are also carried out under various Reynolds numbers Re ranging from 0.01 to 1 for two Deborah numbers De=10 and 20 above the critical value De=2 for the negative wake.

The simulated flow fields are shown in Figs. 10 and 11. Clearly, the opening angle θ decreases with increasing Re. Quantitative measurements of θ as a function of Re for both De=10 and 20 in (Fig. 12) confirm qualitatively the experimental tendency [27]. In particular, the decrease of θ is also limited for large Re by a finite asymptotic value that depends on the Deborah number.

CONCLUSIONS

The rise of a rigid sphere in a linear viscoelastic fluid of Maxwell type is studied by means of lattice Boltzmann simulations. Two dimensionless numbers are identified as central to the existence of the negative wake as well as its form: the Deborah number De and the Reynolds number Re. The elastic origin of the negative wake is clearly proved by the necessary requirement for the Deborah number De$>$2. Moreover, the simulation results show that the opening angle θ of the upward flow cone surrounding the negative wake decreases from 180° for small Re toward an asymptotic value for large Re. The complete flow fields obtained by the LB simulations capture satisfactorily the main experimental features of bubbles rising in viscoelastic fluids without any fitting parameter. It is noteworthy that such complete and complex flow fields around a sphere under wide ranges of both De and Re are still missing up to date in the literature of numerical simulations in non-Newtonian fluids. Further LB simulations will be focused on the interactions between rising spheres or bubbles with both linear and nonlinear constitutive equations of fluid rheology. Moreover, a fully 3D scheme should be employed to describe the complex flow structure.

ACKNOWLEDGMENT

We would like to thank sincerely Dr. D. d'Humières (LPS, ENS Ulm) for stimulating discussions.

[1] G. G. Stokes, Trans. Cambridge Philos. Soc. **9**, 8 (1851).
[2] O. Hassager, Nature (London) **279**, 402 (1979).
[3] D. Funfschilling and H. Z. Li, Chem. Eng. Sci. **56**, 1137 (2001).
[4] H. Z. Li, Y. Mouline, L. Choplin, and N. Midoux, C. R. Acad. Sci., Ser. IIb: Mec., Phys., Chim., Astron. **324**, 491 (1997).
[5] G. Astarita and G. Apuzzo, AIChE J. **11**, 815 (1965).
[6] G. F. Tiefenbruck and L. G. Leal, J. Non-Newtonian Fluid Mech. **10**, 115 (1982).
[7] M. D. Chilcott and J. M. Rallison, J. Non-Newtonian Fluid Mech. **29**, 381 (1988).
[8] W. J. Lunsmann, L. Genieser, R. A. Brown, and R. C. Armstron, J. Non-Newtonian Fluid Mech. **48**, 63 (1993).
[9] M. B. Bush, J. Non-Newtonian Fluid Mech. **55**, 229 (1994).
[10] J. V. Satrape and M. J. Crochet, J. Non-Newtonian Fluid Mech. **55**, 91 (1994).
[11] D. D. Joseph and J. Feng, J. Non-Newtonian Fluid Mech. **57**, 313 (1995).
[12] P. Singh, D. D. Joseph, T. I. Hesla, R. Glowinski, and T. W. Pan, J. Non-Newtonian Fluid Mech. **91**, 165 (2000).
[13] O. G. Harlen, J. Non-Newtonian Fluid Mech. **108**, 411 (2002).
[14] C. Bisgaard, J. Non-Newtonian Fluid Mech. **12**, 283 (1983).

[15] M. T. Arigo and G. H. McKinley, Rheol. Acta **37**, 307 (1998).
[16] X. Frank and H. Z. Li, Phys. Rev. E **71**, 036309 (2005).
[17] G. Astarita, Ind. Eng. Chem. Fundam. **5**, 548 (1966).
[18] H. Z. Li and X. Frank, Phys. Lett. A **325**, 43 (2004).
[19] M. R. Swift, W. R. Osborn, and J. M. Yeomans, Phys. Rev. Lett. **75**, 830 (1995).
[20] S. Chen and G. D. Doolen, Annu. Rev. Fluid Mech. **30**, 329 (1998).
[21] S. Succi, *The Lattice Boltzmann Equation for Fluid Dynamics and Beyond* (Clarendon Press, Oxford, 2001).
[22] P. Lallemand, D. d'Humières, L. S. Luo, and R. Rubinstein, Phys. Rev. E **67**, 021203 (2003).
[23] S. Gabbanelli, G. Drazer, and J. Koplik, Phys. Rev. E **72**, 046312 (2005).
[24] R. P. Nourgaliev, T. N. Dinh, T. G. Theofanous, and D. Joseph, Int. J. Multiphase Flow **29**, 117 (2003).
[25] L. Giraud, D. d'Humières, and P. Lallemand, Europhys. Lett. **42**, 625 (1998).
[26] A. J. Wagner, L. Giraud, and C. E. Scott, Comput. Phys. Commun. **129**, 227 (2000).
[27] M. Kemiha, X. Frank, S. Poncin, and H. Z. Li, Chem. Eng. Sci. **61**, 4041 (2006).